DOI: https://doi.org/10.37434/tpwj2025.03.01

DETERMINATION OF THE QUANTITATIVE PHASE COMPOSITION OF THE METAL OF WELDED JOINTS OF HIGH-ALLOY STEELS, INCLUDING DUPLEX STEELS

G.V. Fadeeva[1], S.Yu. Maksymov[1], Chuanbao Jia[2], D.V. Vasiliev[1], A.A. Radzievska[1]

[1]E.O. Paton Electric Welding Institute of the NASU
11 Kazymyr Malevych Str., 03150, Kyiv, Ukraine
[2]MOE Key Lab for Liquid-Solid Structure Evolution and Materials Processing, Institute of Materials Joining, Shandong University, Jinan 250061

ABSTRACT

The article considers the main techniques and methods available today for quantitative determination of the phase composition of metal in welded joints of high-alloy and duplex stainless steels (DSS). The feasibility of using particular method in different cases is analysed. The article presents the results of the analysis of the influence of cooling rate on the structure and phase composition of weld metal and HAZ during welding of high-alloy chromium-nickel steels and duplex stainless steels. It is shown that due to the influence of high cooling rates, such as during welding in aqueous medium, the amount of ferritic component in the weld metal and deposited metal of high-alloy steels decreases, whereas in the weld metal and HAZ of duplex steels, on the contrary, the amount of austenitic component decreases. This depends on the type of metal solidification. The presented data explain the differences in determining the phase composition of the weld metal and deposited metal at the same alloying during welding in different environments. The main advantages and disadvantages of various techniques and methods for quantitative determination of the phase composition of welded joints of high-alloy and duplex steels are shown.

KEYWORDS: high-alloy chromium-nickel steels, duplex steels, phase composition, austenite, ferrite, cooling rate, methods for quantitative determination of phase composition

INTRODUCTION

The main task in welding high-alloy austenitic steels and duplex stainless steels (DSS) is to ensure conditions that should help mitigating the negative impact of the thermal welding cycle (TWC) on the microstructure and phase composition of weld metal and HAZ of welded joints.

Depending on welding conditions, primarily on the cooling rate, in the temperature range of phase transformations, which is almost the same for both high-alloy austenitic steels and duplex stainless steels and corresponds to the temperature range T = 1450–800 °C for high-alloy austenitic steels and a slightly lower temperature range for duplex stainless steels T = 1300–800 °C, depending on the chemical composition of the metal, a corresponding structure is formed with a certain composition of austenite and ferrite phase components. The microstructure and its phase composition are the most important factors that determine the basic technological and other characteristics, such as mechanical properties and corrosion resistance, as well as resistance to hot crack formation as, for instance, in welding austenitic steels.

The most efficient method to increase the resistance of austenitic welds against the formation of hot cracks is to provide the weld metal with a ferritic component. Producing welds having an austenitic-ferritic structure with the amount of ferrite from 2 to 7–8 % significantly improves the resistance of the weld metal against the formation of hot solidification cracks [1]. The upper limit of ferrite content is limited to the specified amount in the case of operation of products at a temperature above 300 °C [2]. In some cases, to ensure the required corrosion resistance in highly aggressive non-oxidizing environments, the presence of ferritic phase in the weld metal or in the base metal is not allowed [3]. For operation at cryogenic temperatures, stable austenitic chromium-nickel and chromium-nickel-molybdenum steels containing 17–25 % chromium, 8–25 % nickel, and 3–6 % molybdenum are usually used. In these steels, the martensitic transformation is suppressed and the austenitic structure is preserved down to the lowest temperatures (–196 °C). These steels are stable austenitic and, therefore, the content of ferritic component in such welds and in the welded metal is also unacceptable. The welds should have a greater margin of austeniticity compared to the base metal, i.e. the Cr_{eq}/Ni_{eq} ratio should be lower than the Cr_{eq}/Ni_{eq} ratio of the base metal [4].

In duplex stainless steels, the optimum combination of high strength characteristics and corrosion resistance against pitting corrosion and stress corrosion cracking is achieved when the ratio of ferritic and austenitic phases in the metal structure is 1:1, i.e., when the content of each component is 50 %.

Table 1. Ferrite content in welded joint according to standards

Standard description	Ferrite content		
	BM	HAZ	WM
API RP 582 (API A 938 C) [6]	30–65	30–65	30–65
NORSOK M630 D45 [7]	35–55	30–70	
Specification for the oil and gas industry	35–55	< 60–65	< 60

Under the effect of the welding thermal cycle due to the high heating and cooling rates inherent in various types of welding, the original austenite-ferrite phase balance is violated. To maintain this balance, guidelines and standards provide recommendations to ensure the content of austenitic and ferritic components in different parts of a welded joint in the required amounts. The ferrite content in the weld metal and heat-affected zone should be within 25–70 % to ensure the optimum mechanical properties and corrosion resistance [5].

Different fields of operation of high-alloy steel welded joints and industries are governed by regulatory documents and standards, as well as welding process instructions that specify the phase composition of the weld metal and HAZ to ensure the required characteristics and corrosion resistance of a weldment.

Table 1 shows the requirements for ferrite content in a welded joint of duplex stainless steels used in the oil and gas industry.

Many studies have been devoted to the influence of microstructure and austenite/ferrite ratio in duplex stainless steels on the mechanical properties and corrosion resistance of welded joints [8–10].

The corrosion resistance and mechanical properties of welded joints of austenitic, austenitic-ferritic and duplex steels under different operating conditions have their own characteristics and depend on many factors, such as chemical composition, structural heterogeneity, phase composition, etc. Determination of the quantitative phase composition of structural components in the metal of welded joints is of great importance for ensuring the main technological properties of welded structures.

All of the stated above indicates the importance of determining the phase composition of weld metal and HAZ in welding high-alloy steels of austenitic, austenitic-ferritic grades, as well as duplex stainless steels of ferritic-austenitic grade.

Taking into account the relevance of the above material, it is necessary to analyse the basic techniques and methods available today for determining the phase composition of metal in welded joints of high-alloy steels and duplex stainless steels.

THE AIM

of this study is to find out the feasibility of using a particular technique and method for determining the quantitative phase composition, as well as to show, based on experimental data, the effect of cooling rate on the microstructure and phase composition of the welded joint metal during welding in different environments; to show the basic advantages or disadvantages of different techniques and methods for quantitative determination of the phase composition in welding high-alloy steels.

ANALYSIS OF AVAILABLE METHODS FOR QUANTITATIVE DETERMINATION OF THE PHASE COMPOSITION OF WELDED JOINTS

There are several basic methods for determining the phase composition of high-alloy steels of various structural classes, such as Scheffler, Delong, WRC-1992 (FN) and Espy diagram, measurements using ferritometers and feritscopes, manual point counting according to ASTM E562, X-ray diffraction analysis, and image analysis software.

Let us consider each of these methods in more details.

CONSTITUTION DIAGRAMS

To determine the structure of high-alloy welds by their chemical composition, constitution diagrams are commonly used, constructed depending on the content of elements that stabilize austenite and ferrite. To take into account the influence of alloying elements on the structure and phase composition of welds in relation to nickel and chromium, the concepts of nickel equivalent (Ni_{eq}) and chromium equivalent (Cr_{eq}) were introduced, which take into account the influence of other alloying elements in relation to nickel and chromium. The calculated values of Ni_{eq} and Cr_{eq} are used to determine the phase composition of metal on the constitution diagrams.

The type of solidification of the weld metal can also be determined by the pseudo-binary diagram (Fe–Cr–Ni), constructed using the equivalent Cr_{eq}/Ni_{eq} ratio. This ratio in the pseudo-binary diagram (Fe–Cr–Ni) provides important information about the mode of primary solidification and phase transformations during cooling.

Figure 1 shows a pseudo-binary diagram constructed using the equivalent Cr_{eq}/Ni_{eq} ratio [11].

According to the Scheffler [12], Delong [13], WRC-92 (FN) [14] and Espy diagram [15], the phase composition of the weld metal can be determined. The following equations are used to determine Ni_{eq} and Cr_{eq} for the Scheffler, Delong, WRC-92 (FN) and Espy diagram:

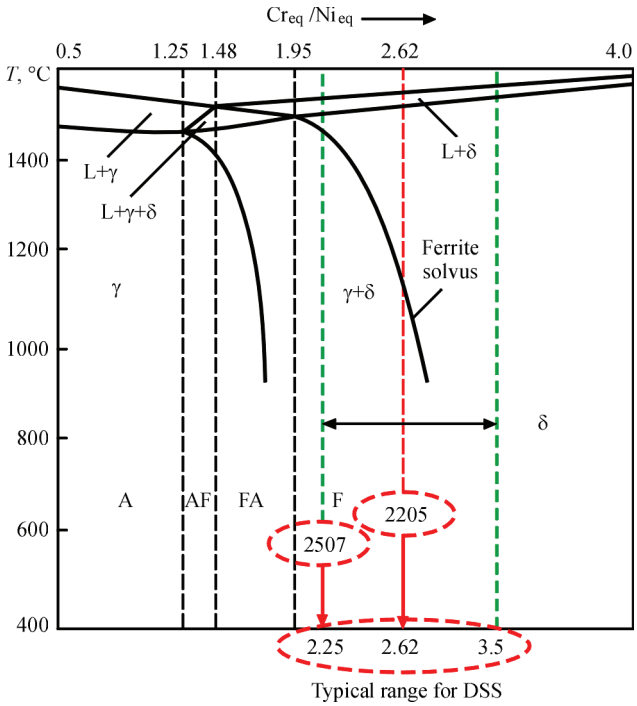

Figure 1. Pseudo-binary (Fe–Cr–Ni) diagram constructed using the equivalent Cr_{eq}/Ni_{eq} ratio [11]

Scheffler diagram (1949)

$$Cr_{eq} = Cr + Mo + 1.5Si + 0/5Nb; \quad (1)$$

$$Ni_{eq} = Ni + 30C + 0.5Mn; \quad (2)$$

Delong diagram (1973)

$$Cr_{eq} = Cr + Mo + 1.5Si + 0.5Nb; \quad (3)$$

$$Ni_{eq} = Ni + 30C + 30N + 0.5Mn; \quad (4)$$

WRC-92 diagram (FN)

$$Cr_{eq} = Cr + Mo + 0.7Nb; \quad (5)$$

$$Ni_{eq} = Ni + 35C + 20N + 0.25Cu; \quad (6)$$

Espy diagram (2005)

$$Cr_{eq} = Cr + Mo + 1.5Si + 0.5Nb + 5V + 3Al; \quad (7)$$

$$Ni_{eq} = Ni + 30C + 0.87Mn + 0.33Cu + 30(N - 0.045). \quad (8)$$

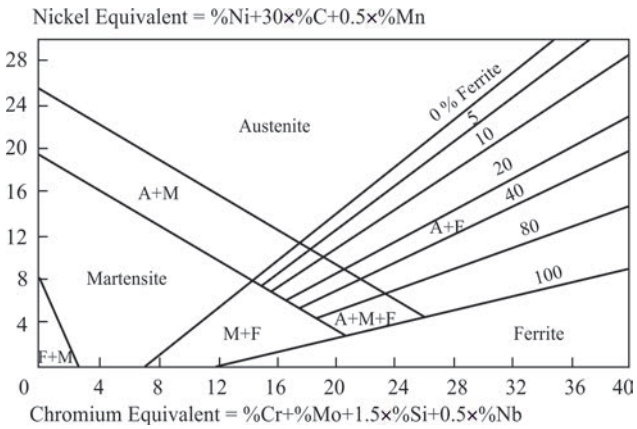

Figure 2. Scheffler constitution diagram [12]

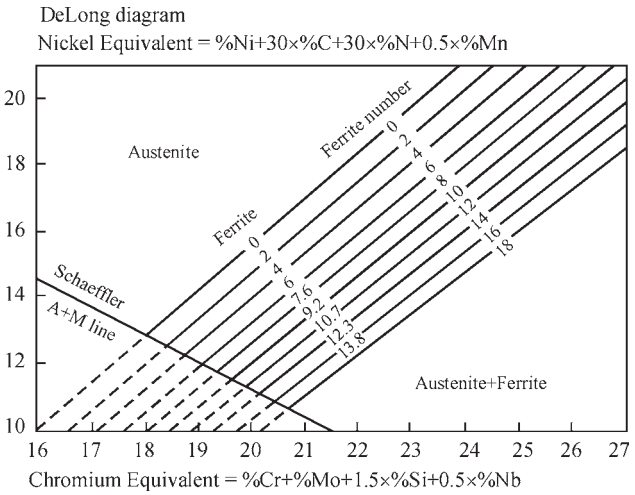

Figure 3. Delong constitution diagram [13]

In addition to equations (1–8), there are other equations for calculating Cr_{eq} and Ni_{eq}, namely (9, 10) [16–18].

$$Ni_{eq} = Ni + Co + 0.1Mn–0.01Mn^2 + 18N + 30C; \quad (9)$$

$$Cr_{eq} = Cr + 1.5Mo + 1.5W + 0.48Si + + 2.3V + 1.75Nb + 2.5Al. \quad (10)$$

Figures 2–4 show the above constitution diagrams.

The cooling rate also affects the type of metal solidification. With its increase, the austenitic region expands during the solidification of austenitic stainless steels at ultra-high cooling rates (Figure 5).

Initially, on the basis of experimental studies, a Scheffler diagram was created to predict the phase composition of weld metal of high-alloy steels of various structural grades for the cooling rate typical of the welding process [12].

With the emergence of nitrogen-containing steels, Delong took into account the presence of nitrogen in the steel and in the weld metal through its contribution to the nickel equivalent [13]. The effect of nitrogen on the austenitic phase is similar to that of carbon. Both alloying elements have the same effect

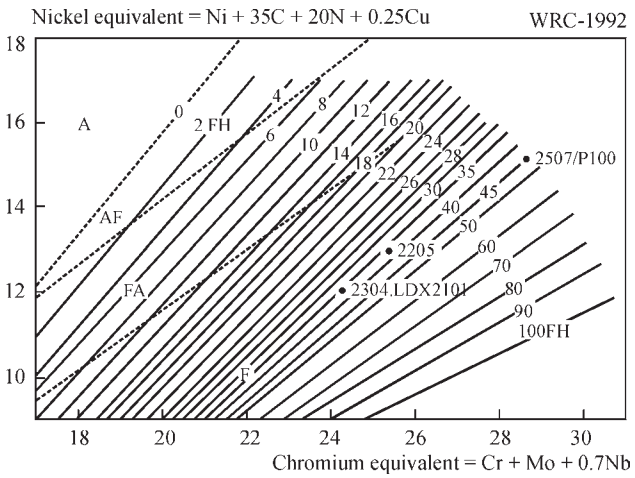

Figure 4. WRC-92 (FN) constitution diagram [14]

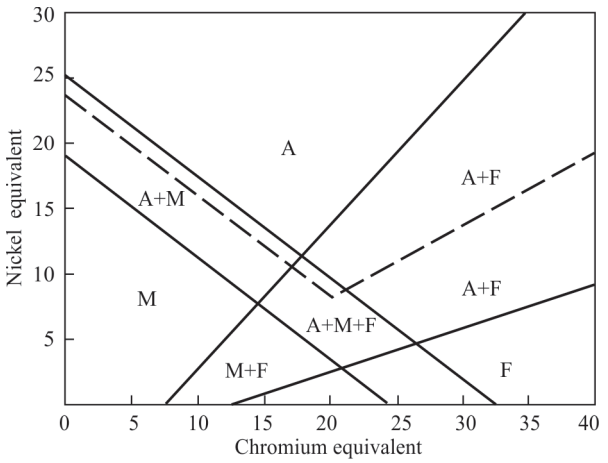

Figure 5. Modified Scheffler diagram for cooling rate of approximately 10^6 K/s [19, 20]

on increasing the stability of austenite, which is determined by the coefficient 30. This formula allows for a more accurate evaluation of the phase composition and microstructure of steels containing nitrogen in higher amounts.

Recently, the Espy diagram has been introduced. This diagram is a modification of the Scheffler diagram and, similar to the Delong diagram, takes into account the influence of nitrogen and other alloying elements. In this case, Cr_{eq} and Ni_{eq} are calculated according to equations (7) and (8) [15].

Analyzing the equations that are used to determine Cr_{eq} and Ni_{eq}, it can be found that for today, there is no unanimous opinion on the equivalent impact of different austenite- and ferrite-forming elements. Some publications provide different coefficients. Thus, the coefficient of ferrite-forming action of molybdenum is in the range from 1 to 2 [1]. There are also different coefficients of impact of the austenite-forming effect of nitrogen, which range from 18 to 30. This indicates that up to this day, the degree of impact of various elements on the structure and phase composition of weld metal is being improved and clarified. This explains that prediction of the phase composition of weld metal using constitution diagrams and determination of Cr_{eq} and Ni_{eq} cannot provide high accuracy when using this method.

The most accurate version for predicting weld metal in welding duplex steels (DSS), recommended by the Welding Research Council (WRC), is the WRC-1992 (FN) diagram [14]. Its use can predict the structure with an accuracy of approximately ±4 ferrite number (FN) when calculating its levels up to 18 FN. The diagram can be used for values of up to 100 FN, which is important for duplex stainless steels.

On the Delong and WRC-92 (FN) constitution diagrams, the amount of ferritic component can be defined as a percentage of ferrite content or as a ferrite number FN. The ferrite number was originally supposed to be a reasonable approximation of the "ferrite percentage" in the metal of a 19-9 or 308 type weld, but later studies show that FN is significantly higher than the "ferrite percentage" in the weld metal. The adoption of an arbitrary "ferrite number" scale is related to the use of measuring instruments and their calibration, which are widely used in foreign measuring instruments — feritscopes. This issue will be discussed in more detail in the next section.

Methods for determining the microstructure and phase composition of weld metal of high-alloy steels of various structural classes using Scheffler, Delong, WRC-92 (FN) and Espy constitution diagrams, as well as according to the pseudo-binary diagram (Fe–Cr–Ni) by calculating Cr_{eq} and Ni_{eq} and their ratio can be successfully used by researchers and developers of welding consumables for prediction when choosing a weld metal alloying system, as well as to determine a welding technology. For a more accurate determination of the phase composition, it is necessary to additionally use other methods.

MEASUREMENTS USING FERRITOMETERS AND FERITSCOPES

Measurement using ferritometers and feritscopes belongs to non-destructive types of testing and quantitative determination of the phase composition of welded joints. The operation of these devices is based on the concept that the ferrite phase (α-phase) and strain martensite (α′-phase) are ferromagnetic, while the austenite phase is paramagnetic.

When using the volumetric method, standard size specimens that are cut out of the test area are magnetized to the state of technical saturation. This is a destructive method. At local magnetic testing, the material is magnetized only at a small area of a product. Most existing modifications of ferritometers that are still in use are based on the local principle of measuring the ferritic component. The local method of magnetic ferritometry is widely used in the non-destructive method of determining the quantitative phase composition due to its efficiency and the ability to determine the content of the ferritic phase directly in a finished product.

The operation of feritscopes used abroad is based on measuring the breakaway force of a permanent magnet from the surface of a specimen. This measurement uses the term "ferrite number" or FN.

The disadvantage of quantitative phase composition measurements using ferritometers and feritscopes is that the measurement is only possible in the weld metal or base metal. It is impossible to measure the

phase composition in the HAZ of a welded joint using these methods due to its small size.

Today, a modern portable Feritscope FMP 30 is available designed for measuring the ferrite content of high-alloy steels of the austenitic-ferritic grade, as well as duplex steels, in which the measurement of the magnetic component can be both in percentage as well as on a scale (FN) [21].

Advantages:

- two measuring ranges;
- switching option for measuring ferrite on the FN scale and as a percentage of ferrite;
- measuring range from 0.15 to 80 % of ferrite, or from 0.15 to 110 FN;
- measurements according to ISO 17655 or Basler Standard;
- calibration specimens are produced based on the international TWI secondary standards that meet the requirements of ISO 8249 and AWS A 4. 2M;
- compliance with the measurement accuracy specified in ANSI/AWS A4. 2M/A 4.2 1997.

MANUAL POINT COUNTING METHOD ACCORDING TO ASTM E 562

This test method describes a systematic manual point counting procedure for statistical evaluation of the volume fraction of an identified phase on metallographic images using a point grid [22]. Although the method of manual point counting is standardized and widely used to determine the quantitative phase composition, it should be recognised that its main disadvantage is the slowness and high labour intensity, operator subjectivity, which depends on his skills, the dependence of the relative measurement accuracy on a number of fields and points, which can lead to imperfect results. Determination of the measured phase by different operators on the same metallographic image can lead to completely different values of the volume fraction of the phase component. This method is very imperfect and its application requires verification and comparison with other methods.

X-RAY DIFFRACTION METHOD OF ANALYSIS

Determination of the phase composition of high-alloy and duplex stainless steels by X-ray diffraction (XRD) analysis is the most contemporary and advanced method.

Advantages of X-ray diffraction (XRD) analysis:

- high accuracy in determining crystal phases;
- phase composition is determined in volume;
- can determine the quantitative ratio of phases in a specimen;
- reveals the exact crystal structure and defects in the crystal lattice;
- ability to analyse small specimens.

Disadvantages:

- XRD requires more expensive specialized and more complex equipment and specimen preparation.

METHOD USING IMAGE ANALYSIS SOFTWARE

There are several powerful types of software for analysing steel microstructures. The most popular and effective of them are:

1. Imagel/Fiji is a free, open source image analysis software. It is widely used in materials science for microstructure analysis, including grain size measurement, phase analysis, and statistical processing.

2. MIPAR™ is a software package specifically designed for the analysis of material microstructures. It offers advanced features for image segmentation, quantitative phase analysis and microstructure characterisation.

3. Clemex Vision PE is a comprehensive solution for image analysis in materials science. It offers automated tools for analysing grains, particle shape, phase distribution and other microstructure parameters.

4. OLYMPUS Stream, Carl Zeiss Axio Vision, Thermo Scientific™ Phenom Particle X are image analysis software specially developed by microscope manufacturers and used with the respective OLYMPUS, Carl Zeiss, Phenom microscopes for automated analysis of various microstructure parameters.

The following advantages of image analysis software can be noted:

- easier in use and cheaper equipment compared to XRD;
- possibility of visualization and evaluation of microstructure;
- helps in studying morphology and phase distribution.

The disadvantages include:

- accuracy depends on the quality of images obtained (e.g. SEM or optical microscopy);
- less accurate quantitative analysis compared to XRD;
- may be less accurate compared to XRD, especially when detecting small phases or microstructural components;
- probable subjective interpretation of results.

Each of these software has its own advantages and the choice depends on the specific needs of the study, steel grade and microstructure to be analysed, and the availability of the particular software. Comparing these two analysis methods, XRD and software, it can be determined that XRD is suitable for material

Table 2. Impact of nitrogen on the structure of chromium-nickel steels [23]

No.	Chemical composition, wt.%			Standard solubility of nitrogen $S_{N, 1873}$, %	Structural composition	
	Cr	Ni	N		Metallographic evaluation	According to Scheffler without nitrogen
1	21.0	6.0	0.47	0.31	A + 21 % F	A + 13 % F
2	21.0	6.0	0.56		A + traces F	A + 8 % F
3	21.0	6.0	0.61		A	–
4	23.5	6.5	0.42	0.32	A + 10 % F	A + 18 % F
5	23.5	6.5	0.45		A + traces F	A + 17 % F
6	23.5	6.5	0.51		A	A + 14 % F
Notes: A — austenite; F — ferrite.						

Table 3. Chemical composition of steels, wt.%

No	Chemical composition of steels					
	C	Mn	Si	Ni	Cr	N
1	0.08	1.2	0.8	6.0	21.0	0.47
2	0.08	1.2	0.8	6.0	21.0	0.56
3	0.08	1.2	0.8	6.0	21.0	0.61
4	0.08	1.2	0.8	6.5	23.5	0.42
5	0.08	1.2	0.8	6.5	23.5	0.45
6	0.08	1.2	0.8	6.5	23.5	0.51

volume analysis and crystal structure determination, whereas software is useful for surface analysis and phase morphology.

Both methods complement each other and can be used together for a complete analysis of the phase composition and microstructure of high-alloy and duplex stainless steels.

To determine the feasibility of using particular method for determining the quantitative phase composition of the metal of welded joints of high-alloy steels and to compare them with each other, examples from the literature are given.

In [23], the structural phase composition of steels containing nitrogen was evaluated by two methods: metallographic and using Scheffler diagram. In this case, the use of the Scheffler diagram is not quite accurate, since it does not take into account the impact of nitrogen. The kind of metallographic method was not specified. Table 2 shows data on the impact of nitrogen on the phase composition of steel.

Using the data from [23], we made an attempt to find out which of the constitution diagrams, Delong, WRC-92 (FN) or Espy, can most accurately predict the phase composition of nitrogen-containing steels. To calculate Cr_{eq} and Ni_{eq}, it was assumed that the metal contains C = 0.08 wt.%, Si = 0.8 wt.% and Mn = 1.2 wt.%. Table 3 shows the chemical composition of the steels selected for calculation of Cr_{eq} and Ni_{eq} to determine the phase composition.

To determine the phase composition according to the Delong constitution diagram, Cr_{eq} and Ni_{eq} were calculated according to equations (3) and (4), for the WRC-92 (FN) diagram — according to equations (5) and (6), and for the Espy diagram — according to equations (7) and (8). The phase composition of steels is shown in Table 4.

Table 4. Phase composition of steels

No	Composition of steels									
	Metallographic evaluation [24]	Delong			WRC-92 (FN)			Espy		
		Cr_{eq}	Ni_{eq}	Phase composition F, %	Cr_{eq}	Ni_{eq}	Phase composition F, %	Cr_{eq}	Ni_{eq}	Phase composition F, %
1	A+21 % F	22.2	23.1	A	21.0	18.2	A	21.0	22.15	A
2	A + traces F	22.2	25.8	A	21.0	20.0	A	21.0	24.85	A
3	A	22.2	27.3	A	21.0	21.0	A	21.0	26.35	A
4	A+10 % F	25.0	22.1	A + 2 % F	25.0	17.3	A + 10 % FN	25.0	21.15	A
5	A + traces F	25.0	23.0	A	25.0	17.9	A + 8 % FN	25.0	22.05	A
6	A	25.0	24.8	A	25.0	19.1	A + 6 % FN	25.0	23.79	A

Analysing the data presented in Tables 3 and 4, it can be found that the prediction of the phase composition of steels according to the Delong and Espy diagrams shows almost the same result. These diagrams are modified from the Scheffler diagram, however they consider the impact of nitrogen on the expansion of the austenitic region. The phase composition of steels calculated according to the WRC-92 (FN) diagram differs slightly from the composition based on the metallographic evaluation. The largest difference in the phase composition of steels compared to the metallographic evaluation corresponds to the Scheffler diagram, if the impact of nitrogen on the phase composition is not taken into account. The differences in the determination of the phase composition in the metal by the metallographic evaluation and constitution diagrams are associated with the fact that [23] considers steels with nitrogen content in the greater amount than its solubility in the metal. Only the nitrogen and carbon content being in the solid solution should be taken into account in the constitution diagrams. It should be noted that all constitution diagrams are designed to predict the weld metal of welded joints, i.e. according to the cooling rates inherent in welding. For example, the Scheffler diagram was created on the basis of experimental data during coated electrode welding, i.e. according to manual arc welding technology. Other diagrams were also developed on the basis of experimental data obtained during outdoor welding. In other words, all constitution diagrams were created for weld metal. It can be said that it is not entirely reasonable to expect the results of predicting the phase composition of steels according to constitution diagrams to be identical to the metallographic evaluation.

In [24], the prediction of ferrite content in the weld at welding dissimilar joints of duplex steel DSS 2205 and stainless steel ASS 316 L was studied using Espy and WRC-92 (FN) constitution diagrams. The ferrite content was also measured experimentally using a Fischer FMP30 feritscope. It has been proven that the use of the WRC-92 constitution diagram (FN) to predict the ferrite content in the weld metal in the amount of FN can lead to a deviation of FN of approximately ±8.69 at welding with an input energy of 0.60 kJ/mm and ±3.86 FN with an input energy of 45 kJ/mm. Whereas, the Espy diagram has a deviation of ±2 % from the experimentally measured value using a feritscope. Prediction by the Espy diagram is less dependent on the cooling rate and is more accurate.

This example shows that the use of constitution diagrams to predict the phase composition of weld metal in welding dissimilar steels can be quite successful.

The Scheffler constitution diagram is also used to predict the phase composition of the weld metal in welding dissimilar steels —low-alloyed with austenitic steels [25].

The prediction of weld metal microstructure carried out based on constitution diagrams and calculation of Cr_{eq} and Ni_{eq} does not take into account the effect of cooling rate and, therefore, has rather limited practical application, especially in welding technologies where the cooling rate differs from the usual one, for example, during welding in aqueous medium, electron beam welding or welding in a pulsed mode, etc. Therefore, to check the predicted phase composition of the weld metal, it is appropriate to compare it with the experimental evaluation of the phase composition using ferritometers or feritscopes.

In [10], the ferrite content in the HAZ of duplex stainless steel 2205 was studied using the manual point counting method in accordance with ASTM E 562 standard [22]. It was noted that the measurement of ferrite in the base metal and in the weld metal using ASTM E 1245 standard [26] usually gives equivalent results compared to the manual point counting method. Determination of the maximum ferrite content in HAZ by this method is complicated. ASTM E 562 is a reference for measuring phases (austenite and ferrite), but does not specify the exact magnification for metallographic examination. Depending on the magnification level, the ferrite content in HAZ shows different results: at a magnification of ×400, the ferrite content is 48 %, at a magnification of ×1000, the ferrite content is determined to be 76 %, i.e., it differs by 1.5 times. Therefore, a magnification of ×400 is not fully representative, whereas a magnification of ×1000 is more suitable for evaluation of the ferrite content in HAZ. In other words, the interpretation of the ferrite content is highly dependent on the operator's skills. The manual point counting method using the grid methodology determines the ferrite content from 50 to 75–80 % for one and the same microstructure.

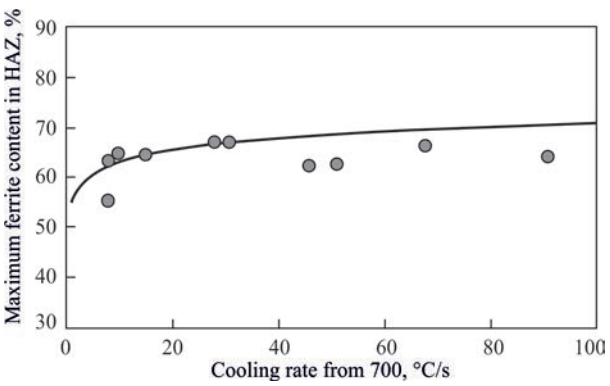

Figure 6. Influence of the measurement procedure on the ferrite content in the HAZ of duplex steel 2205 [10]

Table 5. Ferrite content in weld metal [27]

No	Welding methods	Feritscope (EFN)	Metallographic evaluation, %
1	Electric arc welding with W-electrode	104	78
2	Electric arc welding with W-electrode with additional Ni filler	74	58
3	Electron beam welding	114	86
4	Electron beam welding with additional Ni filler	80	61

Table 6. Phase composition of HAZ modelled at different cooling rates in the temperature range T = 1300–800 °C

HAZ cooling rate, °C/s	Phase fraction, %		
	δ-ferrite	γ-austenite	Excess phase (fine)
Base metal	52.000	48.000	–
8.21	57.499	38.674	3.236
81.70	64.644	30.268	3.746
165.85	67.696	20.965	8.606
320.51	68.848	17.733	13.437

Table 7. Quantitative phase composition and crystal lattice parameters of phase components in the welded joint

Examination area	Method for determining the phase composition	Phase component, %			
		δ-Fe		γ-Fe	
		Content	Lattice period, nm	Content	Lattice period, nm
Weld metal	X-ray diffraction phase analysis	19.4	0.2889	80.6	0.3607
	MIPAR	19.0	–	81.0	–
Base metal	X-ray diffraction phase analysis	52.8	0.2886	47.2	0.3614
	MIPAR	52.0	–	48.0	–

Figure 6 shows the effect of the measurement procedure on the ferrite content in the HAZ of duplex steel 2205. The measurements were carried out according to ASTM E 562.

I.e., this method is very imperfect according to ASTM E 562.

In [8], different welding technologies are compared: electron beam welding, which is characterized by high cooling rates, and electric arc welding with a W-electrode in shielding gas. The ferrite content in the weld metal was measured using a Fisher Feritscope (based on the expanded ferrite number EFN) and the metallographic method of manual point counting. Table 5 shows the measurement results.

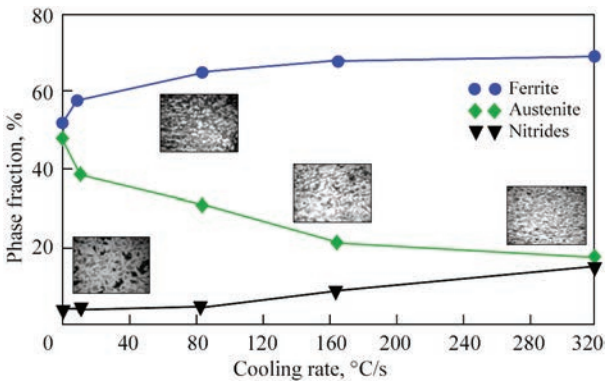

Figure 7. Phase composition of HAZ in the duplex steel depending on the cooling rate in the temperature range of 1200 (1300)–800 °C

It has been proven that the ferrite content in electron beam welding is higher than in electric arc welding with a W-electrode, both with and without an additional nickel filler. This is explained by faster cooling rate in electron beam welding.

The type of primary solidification can be determined by the Cr_{eq}/Ni_{eq} ratio and in accordance with the pseudo-binary Fe–Cr–Ni diagram (Figure 1) [11].

Taking into account the cooling rate ranges used in welding, if $Cr_{eq}/Ni_{eq} \leq 1.5$, the solidification can be austenitic (A) or austenitic-ferritic (A/F). If the ratio is $1.5 \leq Cr_{eq}/Ni_{eq} \leq 2.0$, the solidification will be ferritic-austenitic (F/A). And finally, if $Cr_{eq}/ Ni_{eq} \geq 2.0$, the solidification will be ferritic (F) [27].

EFFECT OF COOLING RATE ON PHASE COMPOSITION DURING WET UNDERWATER WELDING OF DUPLEX STEELS (DSS) 2205 (EXPERIMENTAL DATA)

The results of preliminary studies were borrowed from [28]. Table 6 shows numerical values of the phase composition of HAZ, and Figure 7 shows a

graphical representation of the phase composition of HAZ depending on the cooling rate.

Figure 7 shows the changes in the volume fractions of the phase components of ferrite, austenite, and excess phase (probably the precipitation of chromium Cr_2N nitrides) depending on the cooling rate in the modelled HAZ of the duplex steel in the temperature range T = 1300–800 °C, determined using the MIPAR image analysis software.

A study of the quantitative determination of the phase composition of the welded joint was carried out by two methods: X-ray diffraction analysis and using MIPAR software. The determination of the phase composition was carried out using a Rigaku Ultima IV X-ray diffractometer. Table 7 shows the quantitative phase composition and crystal lattice parameters of the phase components in the weld metal.

The difference in the values of determining the quantitative phase composition can be explained by the fact that the X-ray diffraction analysis method determines the phase composition in volume percents and MIPAR — in wt.%.

CONCLUSIONS

1. The basic methods for determining the quantitative phase composition of the metal of welded joints of high-alloy steels are considered and analysed, and the advantages and disadvantages of a particular method are given.

2. The choice of research method depends on the task according to which it is necessary to determine the phase composition.

3. Prediction of the phase composition of weld metal using constitution diagrams is appropriate for those welding technologies that are characterized by slow cooling of weldments in air.

4. Constitution diagrams do not take into account the cooling rate during welding and, in the cases of high performance welding methods or conditions different from free cooling of weldments in air, introduce a significant error in the determined phase composition.

5. The phase composition of the HAZ in the welded joint can be determined by XRD or by using software.

6. The most imperfect and at the same time very subjective method is manual point counting according to ASTM E562.

REFERENCES

1. Kakhovsky, N.I. (1975) *Welding of high-alloy steels.* Kyiv, Tekhnika [in Russian].
2. Kopersak, N.I. (1963) Influence of alloying elements on 475° brittleness of austenitic-ferritic deposited metal. *Avtomaticheskaya Svarka*, **7**, 15–20 [in Russian].
3. Belinsky, A.L. et al. (1970) *About corrosion resistance of pure austenitic steel grade OKh17N16M3T.* In Coll.: Protection of Metals, Vol. 6, Issue 1. Moscow, Nauka [in Russian].
4. https://uas.su/books/newmaterial/722/razdel722.php
5. Labanowski, J. (1997) Duplex steels — New material for chemical processing industry. *Eng. and Chemical Equipment*, **2**, 3–10.
6. API 582–09: *Welding quidelines for the chemical, oil, and gas industries*.
7. Norsok M-630, Edition 6. October 2013. *Material data sheets and element data sheets for piping*.
8. Muthupandi, V., Srinivasan, P.B., Seshadri, S.K., Sundaresan, S. (2003) Effect of weld metal chemistry and heat input on the structure and properties of duplex stainless steel welds. *Mater. Sci. and Eng.*: A, 358(**1–2**), 9–16. DOI: https://doi.org/10.1016/S0921-5093(03)00077-7
9. Liou, H.-Y., Hsieh, R.-I., Tsai, W.-T. (2002) Microstructure and pitting corrosion in simulated heat-affected zones of duplex stainless steels. *Materials Chemistry and Physics*, **74**, 33–42. DOI: https://doi.org/10.1016/S0254-0584(01)00409-6
10. Higelin, A., Manchet, S.L., Passot, G. et al. (2022) Heat-affected zone ferrite content control of a duplex stainless steel grade to enhance weldability. *Welding in the World*, **66**, 1503–1519. DOI: https://doi.org/10.1007/s40194-022-01326-0
11. Verma, I., Taiwade, R.V (2017) Effect of welding processes and conditions on the microstructure, mechanical properties and corrosion resistance of duplex stainless steel weldments — A review. *J. of Manufacturing Processes*, **25**, 134–152. DOI: https://doi.org/10.1016/J.JMAPRO.2016.11.003
12. Schäffler, A.L. (1949) Constitution diagram for stainless steel weld metal. *Metal Progress*, **56**, 680–680.
13. Delong, F.A. (1973) Ferrite determination in stainless steel weld metal. *Welding J.*, 52(**5**), 210-s–214-s.
14. Kotecki, D.I., Siewert, P.A. (1992) WRC-1992 constitution diagram for stainless steel weld metals: A modification of the WRC-1988 diagram. *Welding J.*, 71(**5**), 171–178.
15. Lippold, J.C., Kotecki, D.J. (2005) *Welding Metallurgy and Weldability of Stainless Steel*. Wiley, Hoboken, New Jersey.
16. Kolpingon, E.Yu., Ivanova, M.V., Shitov, E.V. (2007) Nitrogen-containing steels of equivalent composition. *Chyornye Metally*, February, 10–12 [in Russian].
17. Pomarin, Yu.M., Bialik, O.M., Hryhorenko, H.M. (2007) *The influence of gases on the structure and properties of metals and alloys.* Kyiv, NTUU KPI [in Ukrainian].
18. Cobelli, P. (2003) *Development of ultrahigh strength austenitic stainless steels alloyed with nitrogen*: Syn. of Thesis for Dr. of *Techn. Sci. Degree*. Swiss Federal Institute of Technology in Zurich.
19. Vicente, A., Silva, P.A.D., Souza, R.L.D. et al. (2020) *The use of duplex stainless steel filler metals to avoid hot cracking in GTAW welding of austenitic stainless steel AISI 316L*. DOI: https://doi.org/10.11606/T.3.2017.tde-05092017-103140
20. Jonson, E., Grabaek, L. et al. (1988) Microstructure of rapidly solidified stainless steel. *Mater. Sci. and Eng.*, **98**, 301–303. DOI: https://doi.org/10.1016/0025-5416(88)90174-7
21. http://www Sales@otec.com.ua
22. (2020) ASTM E 562: *Standard test method for determining volume fraction by systematic manual point count*. West Conshohocken, ASTM.
23. Sheiko, I.V., Grigorenko, G.M., Shapovalov, V.A. (2016) Alloying of steels and alloys with nitrogen from the arc plasma. Theory and practice (Review. Pt.1). *Sovremennaya Elektrometallurgiya*, 122(**1**), 32–37 [in Russian]. DOI: https://doi.org/10.15407/sem2016.01.05
24. Verma, J., Taiwade, R.V., Khatirkar, R.K. et al. (2016) Microstructure, mechanical and intergranular corrosion behavior

of dissimilar DSS 2205 and ASS 316 L shielded metal arc welds. *Transact. Indian Inst. Met.,* **70**, 225–237. DOI: https://doi.org/10.1007/s 2666-016-0878-8
25. Zemzin, V.N. (1966) *Welded joints of dissimilar steels.* Moscow, Mashinostroenie [in Russian].
26. (2023) ASTM E 1245-03: *Standard practice for determining the inclusion or second-phase constituent content of metals by automatic image analysis*. https://cdn.standards.iteh.ai.
27. Vicente, A., Silva, P.A.D, Sadanandan, S. et al. (2020) Study on the effect of nitrogen content and cooling rate on the ferrite number of austenitic stainless steels. *Int. J. of Advanced Eng. Research and Sci.,* 7(**11**), 270–277. DOI: https://doi.org/10.22161/ijaers.711.34
28. Maksymov, S.Yu., Fadeyeva, G.V., Jia Chuanbao, et al. (2024) Influence of cooling rate on the microstructure and phase composition of the HAZ of duplex stainless steel (DSS) 2205 during wet underwater welding. *The Paton Welding J.*, **1**, 3–12. DOI: https://doi.org/10.37434/tpwj2024.01.01

ORCID
G.V. Fadeeva: 0009-0003-8142-0110,
S.Yu. Maksymov: 0000-0002-5788-0753,
Jia Chuanbao: 0000-0002-6028-6528,
D.V. Vasiliev: 0000-0002-4629-162X,
A.A. Radzievska: 0009-0002-7718-9668

CONFLICT OF INTEREST
The Authors declare no conflict of interest

CORRESPONDING AUTHOR
S.Yu. Maksymov
E.O. Paton Electric Welding Institute of the NASU
11 Kazymyr Malevych Str., 03150, Kyiv, Ukraine.
E-mail: maksimov@paton.kiev.ua

SUGGESTED CITATION
G.V. Fadeeva, S.Yu. Maksymov, Chuanbao Jia, D.V. Vasiliev, A.A. Radzievska (2025) Determination of the quantitative phase composition of the metal of welded joints of high-alloy steels, including duplex steels. *The Paton Welding J.*, **3**, 3–12.
DOI: https://doi.org/10.37434/tpwj2025.03.01

JOURNAL HOME PAGE
https://patonpublishinghouse.com/eng/journals/tpwj

Received: 25.09.2025
Received in revised form: 29.10.2025
Accepted: 22.04.2025